

## Experimental Performance Investigation and Case Study of Combined Desalination and Power Generation

<sup>a</sup>Abhijit Date, <sup>a\*</sup>Mahdi Ahmadi, <sup>a</sup>Aliakbar Akbarzadeh, <sup>b</sup>Sayantan Ganguly and <sup>b</sup>M.S. Mohan Kumar

<sup>a</sup> School of Aerospace, Mechanical and Manufacturing Engineering, RMIT University, PO Box 71, Bundoora, Victoria 3083, Australia

<sup>b</sup>Department of Civil Engineering, Indian Institute of Science, Bangalore

<sup>a\*</sup>s3513693@student.rmit.edu.au

**Keywords:** Desalination; power generation; hot water springs; geothermal energy, solar thermal energy; salt affected areas; trilateral flash cycle.

### ABSTRACT

This paper presents experimental performance data of a total flow combined desalination and power generation system. A two-phase flow simple reaction turbine has been used in this system which operates on the trilateral flash cycle. Hot saline water is used as the working fluid. The hot water supply temperature is varied from 80°C to 95°C, while the condenser is maintained at about 35°C to 45°C. This paper examines the concept of using the trilateral flash cycle for combined desalination and power generation from saline water in the salt affected areas using geothermal energy. The basic working principle of the combined desalination and power generation system is presented followed by discussions of the governing equations and the thermodynamics of the proposed system. Experimental setup and the test results are briefly explained to give an idea of the performance of the proposed system in a laboratory scale. Later it is shown how a combined desalination and power generation system can be coupled with conventional solar water heaters to boost the fluid temperature when the geothermal resource is at low temperature. Following the introduction of this concept the preliminary design is presented for combined desalination and power generation plant that would use saline water from hot water springs in the western coast of India and provide drinking water for a small coastal village with 20 houses (i.e. approximately 80 people with drinking water need of around 3 L/day/person). Most of the hot water springs along the western coast of India have temperature of around 60°C and hence possibility of boosting the temperature using bio mass or solar thermal energy will also be explored. Attempts are also made to provide some information on the basic economics of such a system.

### Nomenclature

$A_{TN}$	total turbine nozzle exit area ( $\text{m}^2$ )	$U$	linear velocity of turbine (m/s)
$c_p$	specific Heat Capacity (kJ/kg/K)	$v$	specific volume ( $\text{m}^3/\text{kg}$ )
$g$	acceleration of gravity ( $\text{m/s}^2$ )	$V$	velocity (m/s)
$h$	specific enthalpy (J/kg)	$V_r$	relative velocity (m/s)
$I_T$	mass moment of inertia of the turbine ( $\text{kg/m}^2$ )	$V_a$	absolute velocity (m/s)
$KE$	kinetic energy (J)	$\dot{V}$	volumetric flow rate ( $\text{m}^3/\text{s}$ )
$\dot{m}_{fw}$	mass flow rate of feed water (kg/s)	$\dot{W}_{st}$	shaft power (W)
$P$	pressure (Pa)	$\dot{W}_{ex}$	power extracted (W)
$\dot{Q}$	rate of heat transfer (W)	$\omega$	angular velocity of the turbine (rad/s)
$\dot{Q}_{t-o}$	rate of heat supplied to the turbine (W)	$\left[ \frac{d\omega}{dt} \right]_{acc}$	acceleration of the rotating system ( $\text{m/s}^2$ )
$r$	radius (m)	$\left[ \frac{d\omega}{dt} \right]_{dece}$	deceleration of the rotating system ( $\text{m/s}^2$ )
$R_{Throat}$	radial distance of insert/throat from the centre of turbine (m)	$\frac{d(KE)}{dt}$	rate of change in kinetic energy (J/s)
$R$	mean radius of turbine (m)	$x$	dryness fraction
$S$	entropy (J/K)	$z$	elevation (m)
$s$	specific entropy (J/kg/K)	$\eta_{isen}$	isentropic efficiency (%)
$T_i$	inlet temperature (°C)	$\eta_T$	turbine efficiency (%)
$T_o$	outlet temperature (°C)	$\eta_{HE}$	heat engine efficiency (%)
$T_f$	frictional torque (N.m)	$\rho$	density ( $\text{kg/m}^3$ )
$T_{st}$	shaft torque (N.m)		

### 1. INTRODUCTION

Researchers around the world are developing renewable energy based desalination and power generation systems. At the same time is vast amount of low grade (below 100°C) thermal energy that is currently not well utilized due to lack of technology. Low-temperature thermal energy resources like shallow geothermal, geothermal hot water springs, non-concentrating solar thermal and industrial waste heat could be used for a variety of purposes if appropriate technology is developed.

It is desirable to develop a system that can use low-temperature thermal energy to produce fresh water and power. Separate desalination and power generation systems driven by thermal energy have been developed and studied for several decades [1]. Some researchers have developed co-generation organic heat engine coupled to desalination system [2]. Most research publications report on investigations of thermal desalination systems are based on multi-effect evaporation or multi-stage flash, while the publications related to heat engines are based on the organic Rankine cycle. Thermal desalination systems like multi-effect

evaporation or multi-stage flash and low temperature heat engines that work on trilateral cycle use phenomenon of flashing by decompression of sub-cooled hot saline water. Many researchers have studied flash boiling phenomena for a number of different applications, with most employing two-phase stationary nozzles [3-9]. In 1986, Yoshiro, Hiroichi and Teruo conducted experiments to study flashing of superheated liquid jets of water and ethanol into vacuum chambers through stationary nozzles [5]. Experiments showed that two different patterns were formed depending on the superheat temperature. In 1987, Gopalakrishna, Purushothaman and Lior studied the flash evaporation from a hot water pool [6]. This study was conducted with fresh water and with saline water (3.5% NaCl concentration) for initial temperatures from 25°C – 80°C and flash-down temperature difference from 0.5°C – 10°C. It was found that the flashed mass increases with Jakob number and pool depth. In 1993, Ohta and Fujii used a thin wire in front of the throat of a converging and diverging nozzle to enhance the flashing process [7]. They found that the slip between the vapour and liquid along the diverging section and the maximum non-equilibrium pressure drop at the nozzle throat cause a decline in the nozzle efficiency. They did experiments on stationary nozzles with sub-cooled hot water at 136°C to 148°C.

There are very few occasions when a rotating two phase nozzle has been investigated in the past and till 2009 no one had proposed to use a two-phase rotating nozzle turbine for combined desalination and power generation.

In 1978, Austin and Lundberg first introduced the concept of a total flow impulse turbine for geothermal energy conversion [4]. The results showed that the total-flow impulse turbine can achieve high efficiency and is competitive economically with conventional systems. They showed that the total-flow concept offers the benefit of more efficient utilization of geothermal resources for electric power production. They evaluated several liquid expander designs for low-temperature resources. The program was terminated before complete field testing of prototype system was done. Later other researchers around the world continued development of total-flow system.

For example, in 1982, Elliott investigated a two-phase-flow turbine with two stages of axial-flow impulse rotors [10, 11]. The turbine efficiency with nitrogen-and-water was 78% for water to nitrogen ratio of 0.68 and the turbine efficiency for Refrigerant 22 was estimated to be around 0.89. The recommended turbine design is a two-stage axial-flow impulse turbine followed by a rotary separator for discharge of separate liquid and gas streams and recovery of liquid pressure.

In 1985, Sebestyen studied and recommended single-stage and multi-stage action and reaction turbines of the axial flow type solely for power generation from geothermal sources [12]. It was reported that the major problem was to design a two-phase turbine that is economical as compared to the conventional expanders used in organic Rankine cycles. As the two-phase turbine would have to handle a very large volumetric expansion with a mixture of vapour and fine liquid drop, the turbine should have an aerodynamic design.

In 1985, Demuth conducted a preliminary evaluation of the velocity pump reaction turbine (VPRT) as a total flow expander in a geothermal heat engine [13]. VPRT had an inner and outer turbine, which are straight nozzles with radial outward flow plus a simple reaction turbine with fluid exiting the turbine tangentially at the outer periphery. The geothermal source temperature was 182°C; the condenser temperature was in range of 38°C to 49°C. The theoretical efficiencies were estimated to range from 47% to 100%. While achievable engine efficiencies were estimated to range from 47% to 77%. The authors claimed that due to the high performance and relative simplicity, the VPRT system appears to warrant further investigation towards its use in a well-head geothermal plant.

In 1993, Fabris through a technical report described different techniques to improve the performance of two-phase simple reaction turbine for power generation from geothermal resources [14, 15]. Fabris work is a continuation of the work done by earlier researchers like Austin and Lundberg [4], Elliott [10, 11], Sebestyen [12], and Demuth [13]. Using a one-dimensional two-phase flow nozzle code Fabris explored different curvatures of the nozzle for some of the flow parameters used by Austin and Lundberg [4] in their earlier work. It was found that the optimal change in the shape of the nozzle does not change much with changing flow parameters. For stationary two-phase flow nozzles the optimal shape of the centreline is a straight line as the axial acceleration may be in the order of 10,000g's (gravitational acceleration), while the acceleration due to gravity that is normal to the direction of flow is only 1g which can cause two-phase fluid separation. If a rotating two-phase reaction turbine has straight nozzles then the two-phase fluid may be exposed to lateral separation forces of order of 6000g's that can cause abrupt flashing which would be the main cause of low nozzle/turbine efficiency for such turbines. So a curved rotating two-phase nozzle would perform reasonably better than straight nozzles as the bulk velocity of the mixture leaving the turbine will be higher generating higher reaction thrust. Fabris [15] developed a method of calculation of the optimal curvature of the rotating two-phase flow flashing nozzles. The curvature of the nozzle is calculated in such a way that the lateral separation forces acting on the fluid are theoretically reduced to zero.

In 2009, Zhao, Akbarzadeh and Andrews proposed to use the two-phase reaction turbine and total-flow concept for simultaneous desalination and power generation [16]. This system used flashing of sub-cooled/saturated hot liquid water due to sudden depressurisation through a two-phase flow turbine. Initially a two arm rotor with straight nozzles was used which showed that the turbine had very low efficiency of around 1%, this was due to power loss in vapour drag and two phase flow separation in straight nozzles. In 2012 Date, Alam, Khaghani and Akbarzadeh proposed using combined desalination and power generation using heat from solar pond [17]. The present paper is a continuation of this research and is focused on improving the overall performance of the combined desalination and power generation system. Following the suggestion made by Fabris [14, 15], two curved nozzle two-phase reaction turbines were designed and tested.

## 2. COMBINED DESALINATION AND POWER GENERATION SYSTEM

Complete utilization of thermal energy from sub-cooled or saturated hot liquid water is theoretically possible by expansion through some type of two-phase turbine with high expansion ratio. A two-phase turbine extracts useful energy from sub-cooled/saturated hot liquid water by reducing the internal energy of the water. Combined Desalination and Power generation system (CDP) operated on trilateral flash cycle and a radial outward flow simple reaction turbine is used as an expander in this system. Assuming that the flow of sub-cooled/saturated hot liquid water is free of vapour, even a small depressurisation would cause phase change and create

a two-phase flow with large volume change. Figure 1 shows the schematic of the CDP, sub-cooled/saturated hot saline water enters into a flashing tank through a radial outward flow simple reaction turbine. Initially the pressure inside the flashing tank is between 5-6kPa absolute, this corresponds to water saturation temperature of about 32-36°C. The cooling water inlet temperature of the condenser is maintained between 18°C to 23°C. The sub-cooled/saturated hot liquid saline water ( $>60^{\circ}\text{C}$ ) flash evaporates in the diverging section of the nozzle inside the simple reaction turbine and exits the turbine tangentially from the outer periphery at a high velocity in form of liquid-vapour mixture. The reaction force of this mixture makes the turbine rotate at very high speed; an electric generator can be connected to this turbine to produce electrical power. The vapour part of the mixture flows to the condenser, where it is condensed and removed from the system as fresh water. The liquid part (brine) of the mixture is at higher salinity, which falls to the bottom of the flashing tank and is continuously removed from the flashing tank. The attraction of this system is that it is capable of utilising entire thermal energy content of sub-cooled/saturated hot liquid water for combined desalination and power generation.

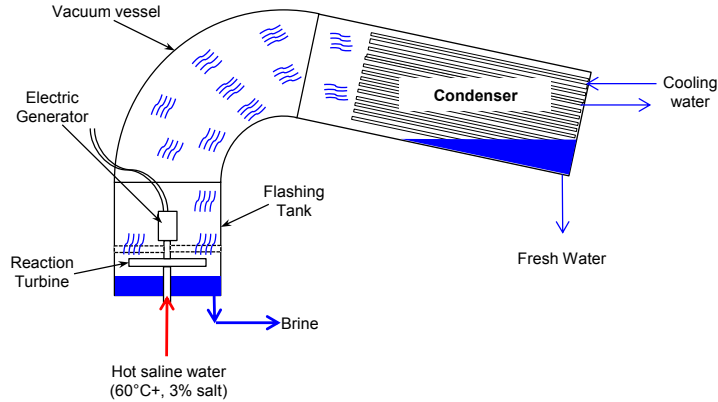


Figure 1 Schematic showing the principle of the CDP system

### 3. THEORETICAL ANALYSIS OF CDP SYSTEM AND SIMPLE REACTION TURBINE

The CDP unit is designed to work under the trilateral flash cycle (TFC) [16-22]. As shown in Figure 2 the compressed liquid water at point 1 is heated close to saturation temperature at point 2 before being feed to the turbine. Then it goes through a pair of nozzle within a simple reaction turbine and ideally experiences an isentropic expansion before the fluid leaves the turbine. Process 2-3 shows the ideal isentropic expansion process which represents maximum power production and highest energy conversion efficiency. Process 2-3" represents adiabatic expansion process with no work output. This is similar to having stationary nozzle and single stage flash desalination. Realistically the process of expansion will be somewhere between the two limits where the end point of the process is shown as point 3' for a real expansion process. One of the objectives of this research is to determine experimentally the position of point 3', in other words to determine the dryness fraction of the fluid as it leaves the turbine and this is done for different turbine configurations.

For an isentropic expansion process, the entropy at point 2 is equal to that at point 3, i.e.  $S_2 = S_3$  or

$S_2 = S_{f2} = S_3 = S_{f3} + xS_{fg3}$ . If the temperature at 3 is known, one can find the corresponding  $S_f$  (specific entropy of saturated fluid) and  $S_{fg}$  (specific entropy of evaporation). Hence the dryness fraction at point 3 can be calculated as  $x = (S_3 - S_{f3})/S_{fg3}$ . Once the dryness fraction is known the enthalpy of the fluid leaving the isentropic turbine can be estimated.

Similarly if the real temperature at the exit of the turbine (i.e. at point 3') is known the dryness fraction of the fluid that leaves the turbine can be estimated and hence the enthalpy of that fluid at the exit of the turbine can be estimated. Knowing this enthalpy at point 3 and 3' one can estimate the isentropic efficiency of the turbine using the following equation.

$$\eta_{isen} = \frac{(h_2 - h_{3'})}{(h_2 - h_3)} \quad 1$$

$$\text{Here, } h_{3'} = h_2 - \frac{\left( \dot{W}_{st} + \frac{1}{2} \times \dot{m}_{fw} \times V_a^2 \right)}{\dot{m}_{fw}} \text{ and } h_3 = h_{f3} + \left( \frac{S_3 - S_{f3}}{S_{fg3}} \right) \times h_{fg3}$$

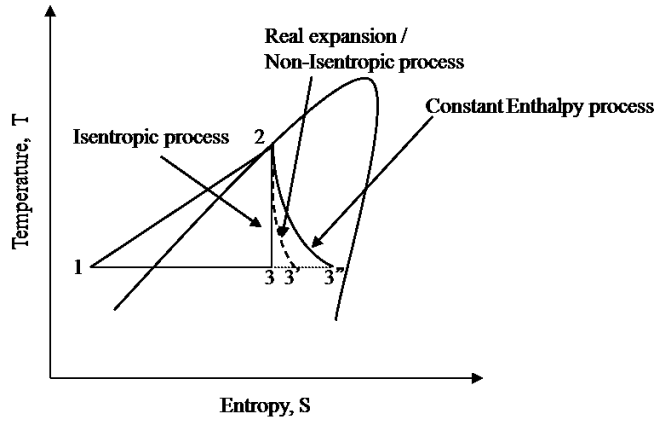


Figure 2 T-S diagram for trilateral cycle of CDP

Further, the relative velocity of the fluid leaving the turbine can be estimated if the feed water mass flow rate and the dryness fraction at point 3 are known:

$$V_r = \frac{\dot{V}_{3''}}{A_{TN}} = \frac{\dot{m}_{fw} \times v_{3''}}{A_{TN}} \quad 2$$

Considering the thermodynamic process that happens in the turbine with one inlet and two exit nozzles as shown in Figure 3, the energy balance equation can be written for the mentioned control volume:

$$\dot{m}_{fw} \times h_i + \frac{1}{2} \times \dot{m}_{fw} \times V_i^2 + \rho \times g \times z_i = \dot{m}_{fw} \times h_o + \frac{1}{2} \times \dot{m}_{fw} \times V_o^2 + \rho \times g \times z_o + \dot{Q} + \dot{W}_{st} \quad 3$$

Here terms with subscript "i" are at inlet to the turbine, while the terms with subscript "o" are at outlet of the turbine. Because of the very slow velocity at the inlet in comparison to the exit velocity,  $V_i$  can be omitted from the equation. In addition, it is assumed that both the inlet and outlet are at same level and so the elevation head is neglected. It is assumed that there is no heat loss to the surroundings as the turbine is in high vacuum environment so  $\dot{Q} = 0$ . Also in the following equation the outlet velocity is called as absolute velocity of the fluid leaving the turbine  $V_o = V_a$ . For the turbine to have maximum efficiency it is expected that the absolute velocity of the fluid leaving the turbine be minimum, i.e. kinetic energy lost with the fluid leaving the turbine be at a minimum.

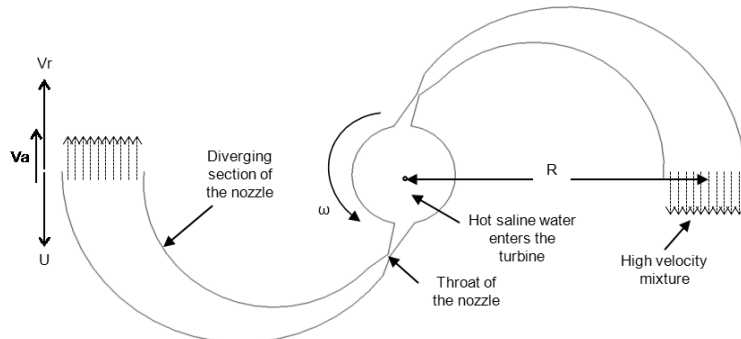


Figure 3 Schematic of the outward radial flow reaction turbine rotor used in CDP

$$\dot{m}_{fw} \times (h_i - h_o) = \frac{1}{2} \times \dot{m}_{fw} \times V_a^2 + \dot{W}_{st} \quad 4$$

In equation 4 the mechanical power output from the turbine  $\dot{W}$  is considered to be a function of rotational torque and the angular velocity and is shown by following equations:

$$\dot{W}_{st} = T_{st} \times \omega = \dot{m}_{fw} \times V_a \times R \times \omega \quad 5$$

$$V_a = V_r - R \times \omega \quad 6$$

$$\dot{W}_{st} = \dot{m}_{fw} \times R \times \omega \times \left( \sqrt{R^2 \times \omega^2 + 2 \times (h_i - h_o)} - R \times \omega \right). \quad 7$$

Initially when the turbine is stationary, the mass flow rate and hence the relative velocity of the fluid exiting the turbine are only dependent on the change in enthalpy between inlet and exit. But as the turbine starts to rotate the mass flow rate increases due to the centrifugal pumping effect and hence the optimum exit nozzle area changes with angular velocity of the simple reaction two-phase turbine as shown by the following equations.

$$V_r = \sqrt{R^2 \times \omega^2 + 2 \times (h_i - h_o)} \quad 8$$

The overall efficiency is represented as the mechanical power output divided by the total thermal energy input to the CDP system. The mechanical efficiency is defined as the ratio of mechanical power divided by the rate of change of thermal energy between inlet and exit of the turbine shown by following equations.

$$\eta_{HE} = \frac{\dot{W}_{st}}{\dot{Q}_H} = \frac{\dot{m}_{fw} \times R \times \omega \times \left( \sqrt{R^2 \times \omega^2 + 2 \times (h_i - h_o)} - R \times \omega \right)}{\dot{m}_{fw} \times C_p \times (T_i - T_o)} \quad 9$$

$$\eta_T = \frac{T_{st} \times \omega}{\dot{m}_{fw} \times \Delta h} = \frac{T_{st} \times \omega}{T_{st} \times \omega + \frac{1}{2} \times \dot{m}_{fw} \times V_a^2} \quad 10$$

#### 4. TEST SET-UP AND PROCEDURE

As shown in Figure 4, the experimental set-up of CDP system has a 500 mm diameter flashing tank, which accommodates the turbine and is maintained at an absolute pressure of about 6 kPa. The turbine is supported with three high precision radial bearings and the shaft that is directly connected to the turbine is brought out of flash tank for speed and torque measurement, here mechanical seals are used to prevent air leakage into the flashing tank. The feed water is pumped through two flat plate heat exchangers connected in series. The water pump is used to prevent water from boiling when heated above 100°C. Here the feed water is heated using steam at 160°C generated by a 150kW steam generator. To control the feed water temperature the steam flow through heat exchanger is manually regulated. Extra steam produced by the steam generator is bleed off. The volume flow rate of feed water is measured before it gets heated in the flat plate heat exchanger; here a vortex-type flow sensor manufactured by Grundfos is used to measure the flow rate. The temperature of the feed water is measured just before the inlet to the rotary shaft of the CDP system. It is very difficult to maintain a constant feed water temperature, when the feed water heated above 100°C; the manual regulation of steam flow is very difficult and causes frequent fluctuation. Existing steam generator was modified to supply hot liquid water at temperatures above 100°C. A shell-and-tube type configuration was used for the condenser and cooling water supply was used for condensing the water vapour produced in the CDP system.

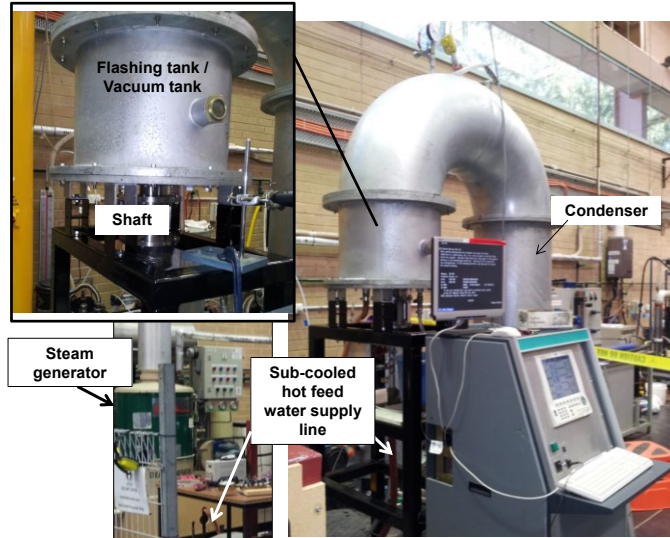


Figure 4 Combined desalination and power (CDP) generation system

During the experiments, the following parameters were continuously monitored from the beginning of each test: temperature of hot feed water, volume flow rate of the feed water, pressure inside the flashing tank and rotational speed of the turbine i.e. acceleration and deceleration of the turbine.

Mechanical power produced by the turbine for a certain rotational speed is the sum of the frictional power loss (includes rolling resistance in bearings and turbine drag), change in kinetic energy and the shaft power that is extracted:

$$\dot{W}_{st}(\omega) = T_f(\omega) \times \omega + \frac{d(KE)}{dt} + \dot{W}_{ex}. \quad 11$$

Here,  $\dot{W}_{st}(\omega)$  represents the power produced by the turbine as a function of the angular speed,  $T_f(\omega)$  represents the sum of frictional torque as a function of angular speed, i.e. dynamic frictional torque. And  $KE$  represents the kinetic energy of the rotating turbine and  $\dot{W}_{ex}$  represents the power that is extracted from the shaft.

The frictional torque varies with the rotational speed and can be estimated by measuring the deceleration of the turbine and shaft assembly under zero load condition. The total power produced during the deceleration is equal to zero. No power is extracted so the frictional power loss is equal to the loss in the rate of kinetic energy:

$$T_f(\omega) \times \omega = -\frac{d(KE)}{dt} = \left[ \frac{d(KE)}{dt} \right]_{deceleration}. \quad 12$$

The kinetic energy can be estimated from the following equation:

$$KE = \frac{\omega^2}{2} \times I_T \quad 13$$

$$\left[ \frac{d(KE)}{dt} \right]_{acc} = I_T \times \omega \times \left[ \frac{d\omega}{dt} \right]_{acc} \quad \text{Or} \quad \left[ \frac{d(KE)}{dt} \right]_{dece} = I_T \times \omega \times \left[ \frac{d\omega}{dt} \right]_{dece} \quad 14$$

Here  $\omega$  is the angular velocity of the turbine and the term  $I_T$  represents the mass moment of inertia of the turbine and the shaft assembly (i.e. all rotating components).

Therefore the dynamic frictional torque can be estimated using the following equation:

$$T_f(\omega) = -\frac{1}{\omega} \times I_T \times \omega \times \left[ \frac{d\omega}{dt} \right]_{dece} = I_T \times \left[ \frac{d\omega}{dt} \right]_{dece} \quad 15$$

The above equation simply states that the value of dynamic frictional torque for any  $\omega$  can be found from the product of the mass moment of inertia of the rotating system and the rate of change of the angular velocity of the rotor in a deceleration test. In the present study the mass moment of inertia " $I_T$ " of the turbine shaft assembly is experimentally found using spring steel cable and calibrating mass method. Therefore the gross shaft power produced by the turbine at any angular speed is estimated using the following equation:

$$\dot{W}_{st}(\omega) = I_T \times \omega \times \left[ \frac{d\omega}{dt} \right]_{dece} + I_T \times \omega \times \left[ \frac{d\omega}{dt} \right]_{acc} + \dot{W}_{ex} \quad 16$$

## 5. TURBINE UNDER INVESTIGATION

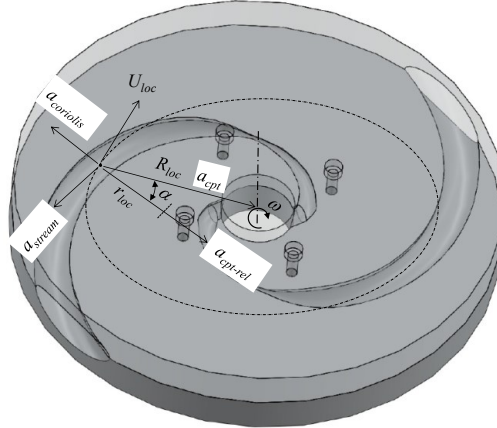


**Figure 5 Localised lateral acceleration forces acting on a particle of fluid flowing within rotating turbine**

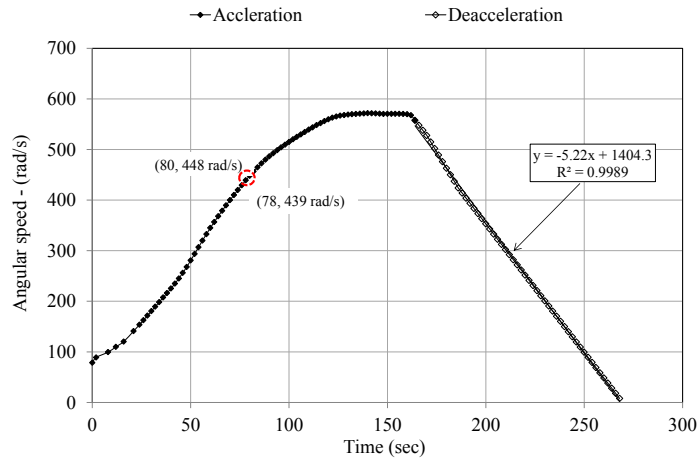
The nozzle curvature of the turbine under investigation was designed based on the suggestions made by Fabris in 1993 patent [14]. Figure 5 illustrates the different acceleration components that are acting on a particle of fluid. The lateral acceleration components that tend to separate the two phases of the fluid are coriolis acceleration  $a_{coriolis}$ , centripetal acceleration relative to motion  $a_{cpt-rel}$  and centripetal acceleration with respect to the centre of the turbine  $a_{cpt}$ . While the turbine is stationary these three acceleration components do not exist and the largest acceleration component is due to the change in the relative motion of the fluid within the nozzle  $a_{stream}$ . To estimate the optimal curvature of the two-phase rotating nozzle the pressure drop along the length of the diverging nozzle is assumed to be linear. And the change in relative velocity of fluid along the length of nozzle is also assumed to be linear. The maximum relative velocity at the exit of the nozzle is calculated assuming an isentropic efficiency of 100% for the turbine geometry and proposed test conditions [23]. In theory, the two phases will not separate if the lateral acceleration components balance each other and there is zero resultant lateral acceleration. The curvature of the nozzle for the second turbine is estimated through an extensive iterative process described by Fabris [14], using the following acceleration balance equation. The operating rotational speed to estimate the curvature of the nozzle of the second turbine is assumed to be 20,000rpm.

## 6. EXPERIMENTAL RESULTS

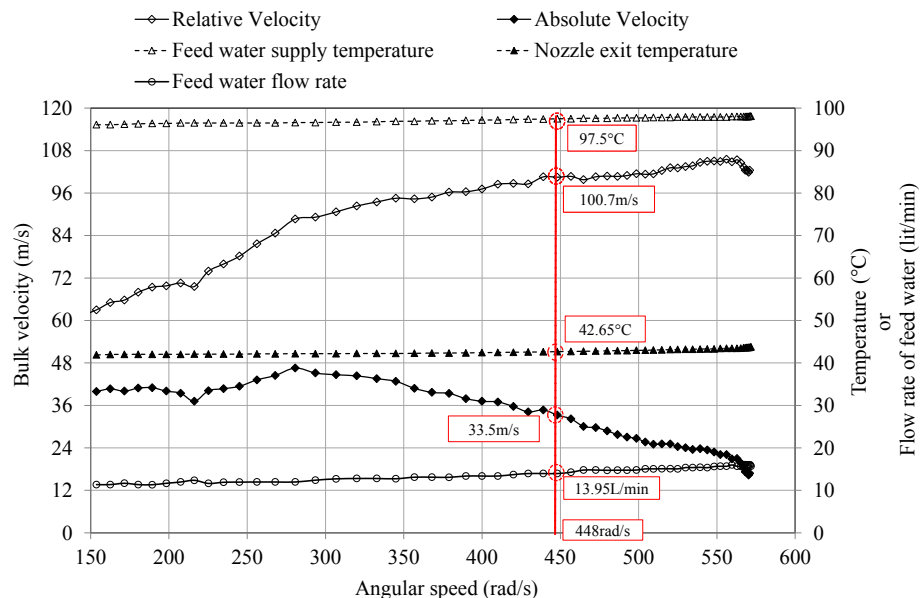
Using the test procedure discussed in the earlier section this turbine was tested for a range of feed water supply temperatures. For all tests the turbine was allowed to accelerate to the maximum rotational speed while the driving temperature difference was tried to be maintained constant. The turbine was allowed to decelerate from the top speed by stopping the feed water supply. The acceleration and deceleration rates were monitored, recorded and analyzed to estimate the gross shaft power produced by the turbine using equation 16.

Figure 6 shows the acceleration and deceleration curves for the turbine with feed water temperature maintained below 100°C. It should be noted that the slope of deceleration curve is directly proportional to the dynamic frictional losses present in the rotary

system that exert load on the turbine. It can be seen from Figure 6 that the slope of deceleration is around  $5.2\text{rad/s}^2$ . The main frictional load is due to bearings and mechanical seal, while the load exerted by the mechanical seal is a function of pressure difference, rotational speed and operating temperature.



**Figure 6 Experimental acceleration and deceleration curves with feed water supply temperature below 100°C during first test**



**Figure 7 Experimental estimations of relative and absolute velocity, feed water flow rate and nozzle exit temperature for test with feed water supply temperature below 100°C during first test**

It should be noted that the feed water flow rate and temperature are measured before the fluid enters the rotating turbine shaft and it is still a sub-cooled liquid. It can be seen from Figure 7 that with increase in the rotational speed the mass flow rate of the feed water increases due to centrifugal pumping. At the same time the relative velocity of the working fluid (water) at the exit of the turbine nozzles also increases, while the driving temperature difference is maintained around 55°C. With increase in the rotational speed of the turbine the absolute velocity decreases and hence the torque produced by the turbine decreases. It can be seen from Figure 8 that the maximum shaft power produced by this turbine for feed water temperature of below 100°C is around 525 W at an isentropic efficiency of around 16%. The maximum isentropic efficiency is estimated to be around 17.5%. Although the efficiency of this turbine is still 6 fold lower than ideal isentropic efficiency, it is a big improvement over the previous designs [17, 24]. The average quality of the mixture at the nozzle exit was estimated to be around 0.09434, i.e. average fresh water production of around 1.31 L/min.

With increase in the rotational speed the mass flow rate of the feed water increased which increase vapour production and the cooling load on the condenser. The present condenser has cooling capacity of around 55kW. It was observed that the beyond 13L/min of feed water flow rate the cooling load on the condenser exceeded the condenser cooling capacity and this caused the flashing tank pressure to increase. And hence there was increase in the nozzle exit temperature while the feed water supply (inlet) temperature was constant. This caused drop in the driving temperature difference which in turn caused the shaft power and isentropic efficiency of this turbine to drop.

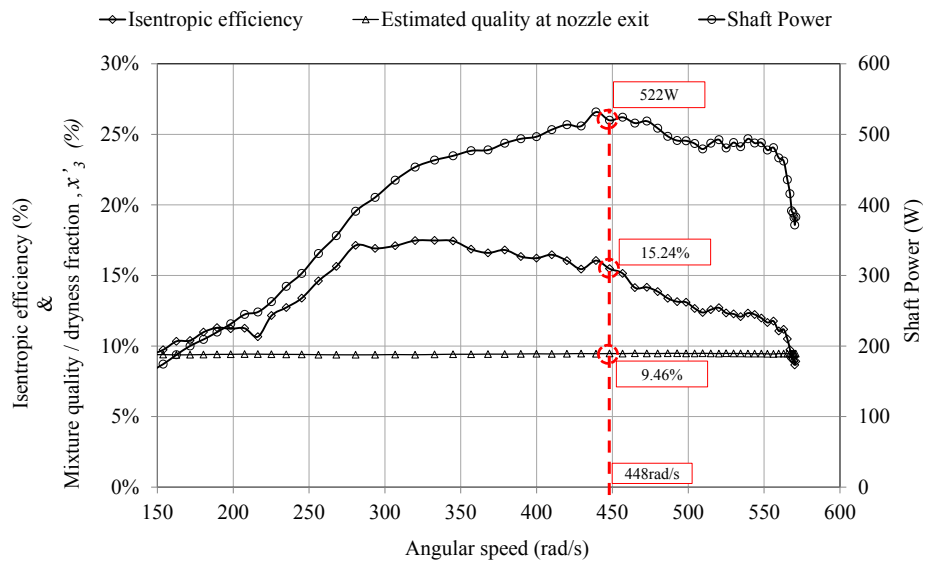


**Figure 8 Experimental estimation of shaft power and isentropic efficiency of the curved nozzle turbine with feed water supply temperature below 100°C during first test**

## 7. CDP COUPLED WITH GEOTHERMAL HOT WATER SPRING

Geo-Solar-Biomass: Combined Desalination and Power Generation System (CDP System)

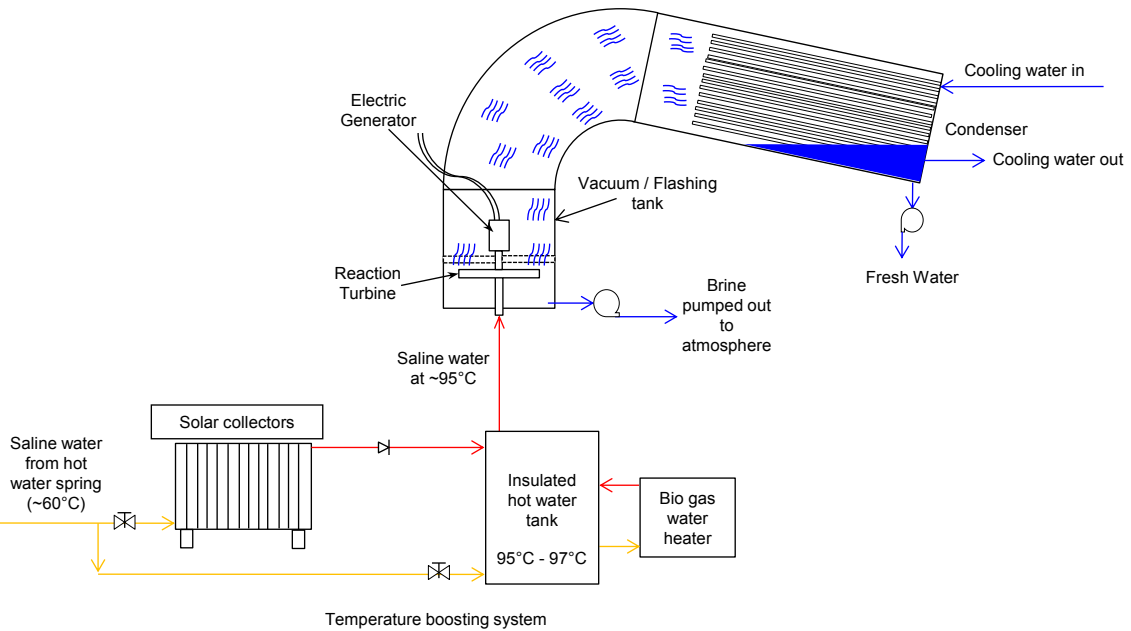


**Figure 9 Schematic of a proposed geo-solar-bio mass CDP system**

Figure 9 shows the schematic of the proposed system that utilizes geothermal energy from natural hot water springs and boosts the temperature with solar thermal and/or biomass heaters. The temperature boosted geothermal water is then supplied to the CDP system that simultaneously produced fresh water and power. Case study presented here investigates the feasibility of using CDP system to supply drinking water and power for a small remote community on the western coast of India with access to natural geothermal hot water spring at average 60°C temperature. It is assumed that this community has 20 houses with 4 people in each house and with drinking water need of around 3L/day/person. Therefore the daily 0.24m<sup>3</sup> of drinking water must be produced by the CDP system.

Based on the experimental results the fresh water recovery rates from the CDP system are around 9% when the inlet temperature is around 95°C and the condenser is around 35°C. So the volume of feed water required to produce 0.24m<sup>3</sup> of fresh water will be around 2.7m<sup>3</sup>. If it is assumed that the system operates for 24hours then the feed water mass flow rate will be around 0.032kg/s at initial temperature of 60°C. The rate of thermal energy required to boost the temperature of the feed water from 60°C to 95°C will be around 4.7kW. So the total energy required per day to boost the temperature of the feed water is around 390MJ<sub>t</sub> (around 108kWh<sub>t</sub>). For this case study it is assumed that 4 evacuated tube solar collector panels with each having effective solar collection area of around 2.7m<sup>2</sup> are used. It is assuming that these solar evacuated tube collectors have 40% efficiency. With peak sun hours of around 5.5hrs in western coast of India the total energy that these 4 solar collectors can collect will be around 85MJ<sub>t</sub> per day. So around 305MJ must be supplied by the bio gas water heater to be able to boost the temperature of the feed water to 95°C. Bio gas

water heater operates when the temperature of the feed water stored in the insulated tank falls below 95°C. This system can produce around 1.7kWh/day of electrical energy in addition to the 0.24m<sup>3</sup> of fresh water. Approximate cost of such a system will be around AU\$6000.

## 8. CONCLUSION

A new reaction turbine design with curved nozzles made from two grooved plates has been described, which is easy to manufacture using a three-axis milling machine. Experiments with below 100°C feed water supply temperatures were carried out to estimate the performance characteristic of the proposed curved nozzle profile turbine. The turbine had outer diameter of 300 mm with two nozzles having throat diameter of 2 mm and nozzle exit diameter of 25 mm (i.e. total nozzle exit area of 981 mm<sup>2</sup>). The turbine was placed in flash tank initially maintained under vacuum pressure of around 6 kPa absolute. The experimental results presented in this paper are average bulk values and could be to some extend used for preliminary validation of a computational fluid dynamics model. Experimental estimations had maximum uncertainty of around  $\pm 7\%$ . The acceleration and deceleration test method used in the present study was found to be very simple and effective for testing of CDP system as it does not require electrical generator or mechanical dynamometer to measure the power output.

The results obtained were as follows,

1. When the turbine was supplied with feed water at 97.5°C the turbine had a maximum isentropic efficiency of around 17% and the maximum shaft power was around 525W. The average feed water flow rate was around 13.95L/min Average fresh water production for first test was measured to be around 1.22 L/min.
2. It is observed that the turbine efficiency increases with increase in the turbine rotational speed. But with the present experimental set-up the turbine speed water limited to around 6000rpm due to following reasons,
  - High mechanical frictional load due to mechanical seals require higher torque to overcome this friction and hence speed is limited.
  - At high speed there is sharp increase in the feed water flow rate that upsets the balance of heat supply to the CDP and heat removed from CDP which caused the pressure in the flash tank to rise and hence reduces the driving temperature and in turn slows down the turbine speed.

Influence of higher rotational speeds on the performance of the turbine and this could be achieved by having large condenser which can handle the cooling loads even at higher rotational speed.

Schematic of geothermal hot water spring boosted with solar thermal and biomass and coupled with CDP has been proposed and the preliminary estimates show that such a system may have the potential for large scale application and hence need further investigation.

It should be noted that condensation of water vapour and removal of non-condensable gasses is very critical for optimal operation of CDP. And as a rule of thumb the future researchers and/or CDP system designers should make sure they use a condenser with cooling capacity at least twice the required cooling load.

## REFERENCES

1. Li, C., Y. Goswami, and E. Stefanakos, *Solar assisted sea water desalination: A review*. Renewable and Sustainable Energy Reviews, 2013. **19**(0): p. 136-163.
2. Austin, A.L., *The LLL geothermal energy program a status report on the development of the total-flow concept*, A.W. Lundberg, Editor 1978, Livermore, Calif.: Dept. of Energy Lawrence Livermore Laboratory ;.
3. Brown, R. and J.L. York, *Sprays formed by flashing liquid jets*. AIChE Journal, 1962. **8**(2): p. 149-153.
4. Austin, A.L. and A.W. Lundberg, *Lawrence Livermore Laboratory geothermal energy program. A status report on the development of the Total-Flow concept*, 1978. p. Medium: ED; Size: Pages: 77.
5. Kitamura, Y., H. Morimitsu, and T. Takahashi, *Critical superheat for flashing of superheated liquid jets*. Industrial & engineering chemistry fundamentals, 1986. **25**(2): p. 206-211.
6. Gopalakrishna, S., V.M. Purushothaman, and N. Lior, *An experimental study of flash evaporation from liquid pools*. Desalination, 1987. **65**(0): p. 139-151.
7. Ohta, J., T. Fujii, K. Akagawa, and N. Takenaka, *Performance and flow characteristics of nozzles for initially subcooled hot water (influence of turbulence and decompression rate)*. International Journal of Multiphase Flow, 1993. **19**(1): p. 125-136.
8. Bunch, T.K., A.A. Kornhauser, and M.P. Alexandrian. *Efficiency of a flashing flow nozzle*. in *Energy Conversion Engineering Conference, 1996. IECEC 96., Proceedings of the 31st Intersociety*. 1996.
9. Mutair, S. and Y. Ikegami, *Experimental study on flash evaporation from superheated water jets: Influencing factors and formulation of correlation*. International Journal of Heat and Mass Transfer, 2009. **52**(23-24): p. 5643-5651.
10. Elliott, D.G., *Tests of a two-stage, axial-flow, two-phase turbine*, 1982. p. Medium: ED; Size: Pages: 34.
11. Elliot, D.G., *Theory and tests of two-phase turbines*, 1982. p. Medium: P; Size: Pages: 149.
12. Sebestyen, I., *Design of two-phase turbines and geothermal electric power-plants in Hungary*. Geothermics, 1985. **14**(2-3): p. 229-246.
13. Demuth, O.J., *Preliminary assessment of the Velocity Pump Reaction Turbine as a geothermal total-flow expander*. 1985. Medium: ED; Size: Pages: 7.
14. Fabris, G., *Two-phase reaction turbine*. , 1993: United States.
15. Fabris, G., *Two-phase reaction turbine*, in *Other Information: PBD: 1 Oct 19991999*. p. Medium: P; Size: vp.
16. Zhao, Y., A. Akbarzadeh, and J. Andrews, *Simultaneous desalination and power generation using solar energy*. Renewable Energy, 2009. **34**(2): p. 401-408.
17. Date, A., F. Alam, A. Khaghani, and A. Akbarzadeh, *Investigate the Potential of Using Trilateral Flash Cycle for Combined Desalination and Power Generation Integrated with Salinity Gradient Solar Ponds*. Procedia Engineering, 2012. **49**(0): p. 42-49.

18. Fischer, J., *Comparison of trilateral cycles and organic Rankine cycles*. Energy, 2011. **36**(10): p. 6208-6219.
19. Zamfirescu, C. and I. Dincer, *Thermodynamic analysis of a novel ammonia–water trilateral Rankine cycle*. Thermochimica Acta, 2008. **477**(1–2): p. 7–15.
20. Lai, N.A. and J. Fischer, *Efficiencies of power flash cycles*. Energy, 2012. **44**(1): p. 1017-1027.
21. DiPippo, R., *Ideal thermal efficiency for geothermal binary plants*. Geothermics, 2007. **36**(3): p. 276-285.
22. Öhman, H. and P. Lundqvist, *Theory and method for analysis of low temperature driven power cycles*. Applied Thermal Engineering, 2012. **37**(0): p. 44-50.
23. Vahaji, S., A. Date, S.C. Cheung, J. Tu, A. Akbarzadeh, and M. Oreijah, *Experimental Analysis of Two-phase Flow nozzle for Desalination and Power Generation System*. Procedia Engineering, 2012. **49**(0): p. 324-329.
24. Date, A., A. Khaghani, J. Andrews, and A. Aliakbar, *Experimental performance of a rotating two-phase turbine for initially sub-cooled hot water for combined desalination and power generation: Part A*. Applied Thermal Engineering, 2014. **Submitted**